Clinical Biomechanics 30 (2015) 121–128

Contents lists available at ScienceDirect

Clinical Biomechanics

journal homepage: www.elsevier.com/locate/clinbiomech

Effect of the metastatic defect on the structural response and failure process of human vertebrae: An experimental study

Ron N. Alkalay

Center for Advanced Orthopedic Studies, Department of Orthopedic Surgery, Beth Israel Deaconess Medical Center and Harvard Medical School, 330 Brookline Avenue, Boston, MA 02215, USA

ARTICLE INFO

Article history:
Received 11 July 2012
Accepted 1 October 2014

Keywords:
Pathologic vertebral fractures
Lytic Defects
Experimental
Failure mechanisms

ABSTRACT

Background: Pathologic vertebral fractures are associated with intractable pain, loss of function and high morbidity in patients with metastatic spine disease. However, the failure mechanisms of vertebrae with lytic defects and the failed vertebrae's ability to retain load carrying capacity remain unclear.
Methods: Eighteen human thoracic and lumbar vertebrae with simulated uncontained bone defects were tested under compression-bending loads to failure. Failure was defined as 50% reduction in vertebral body height. The vertebrae were allowed to recover under load and re-tested to failure using the initial criteria. Repeated measure ANOVA was used to test for changes in strength and stiffness parameters.
Findings: Vertebral failure occurred via buckling and fracture of the cortex around the defect, followed by collapse of the defect region. Compared to the intact vertebrae, the failed vertebrae exhibited a significant loss in compressive strength (59%, $p < 0.001$), stiffness (53%, $p < 0.05$) and flexion (70%, $p < 0.01$) strength. Significant reduction in anterior-posterior shear (strength (63%, $p < 0.01$) and stiffness (67%, $p < 0.01$)) and lateral bending strength (134%, $p < 0.05$) were similarly recorded. In the intact vertebrae, apart from flexion strength ($r^2 = 0.63$), both compressive and anterior-posterior shear strengths were weakly correlated with their stiffness parameters ($r^2 = 0.24$ and $r^2 = 0.31$). By contrast, in the failed vertebrae, these parameters were strongly correlated, ($r^2 = 0.91$, $r^2 = 0.86$, and $r^2 = 0.92$, $p < 0.001$ respectively).
Interpretation: Failure of the vertebral cortex at the defect site dominated the initiation and progression of vertebral failure with the vertebrae failing via a consolidation process of the vertebral bone. Once failed, the vertebrae showed remarkable loss of load carrying capacity.

1. Introduction

Annually, up to 1.5 million new cases of cancer are reported in the U.S (American-Cancer-Society, 2012) with thirty to sixty percent of this patient population presenting bony metastasis in the spine (Ratliff and Cooper, 2004; Toma et al., 2007; White, 2006). The migration of cancer cells to the highly vascular vertebrae often results in the destruction of the osseous tissues (Taneichi et al., 1997; Tschirhart et al., 2004; Whealan et al., 2000; Whyne et al., 2003). This pathological process exposes the patients to a high risk of catastrophic failure of the affected vertebra (Lad et al., 2007; Weber et al., 2011), with the resulting fractures often associated with intractable pain, loss of function and increased morbidity (Falicov et al., 2006; Walls et al., 1995; Weber et al., 2011), and in up to 30% of these patients, neurologic compromise from spinal cord compression (Roth et al., 2004; Taneichi et al., 1997). Pathologic vertebral fracture thus represents an important cause of disability with significant clinical and economic implications for the US healthcare system (Coleman, 2001; Lad et al., 2007; Weber et al., 2011).

The deleterious effect of lytic lesions on the risk of vertebral failure was recently demonstrated in an animal model for vertebral lytic metastasis (Hardisty et al., 2012; Hojjat et al., 2010). The occurrence of the lesion resulted in the doubling of compressive strains compared to the control vertebrae with the development of stress concentration at the dorsal aspects of the vertebrae indicating increased structural instability. Retrospective clinical studies have identified defect geometry, destruction of the pedicles, pain, age, anatomic site, lesion type, activity levels and, for thoracic vertebrae, costovertebral joint destruction, as significant risk factors for impending vertebral collapse (Bunting, 1985; Coleman and Stanley, 1994; Fidler, 1981; Taneichi et al., 1997; Weber et al., 2011). Experimental (Whealan et al., 2000; Windhagen et al., 1997, 2000) and computational (Tschirhart et al., 2004, 2006; Whyne et al., 2001, 2003) studies have further established measures of defect size and geometry, defect location within the vertebral body and bone density, to be predictors of vertebral risk of fracture. However, although most often used as a predictor of vertebral fracture risk (Carlson et al., 1995), relative lesion size has been shown to account for only 50% of the variation in vertebral body strength (Taneichi et al., 1997; Tokuhashi et al., 2005). At present, despite this extensive body of work and clinical reports, no clear guidelines have been established to allow prediction of fracture risk (Roth et al., 2004).

E-mail address: ralklay@bidmc.harvard.edu.

http://dx.doi.org/10.1016/j.clinbiomech.2014.10.001
0268-0033/

Critically, the structural mechanisms underlying the initiation and progression of the failure process for vertebrae with uncontained lytic defects remain unclear.

The objectives of this study were twofold: The first was to investigate the effect of an uncontained defect within the body of thoracic and lumbar human vertebrae, on the failure process of the vertebrae in response to compression-flexion loading. Our hypothesis is that *Failure of vertebral cortex in human vertebrae with significant, uncontained, osetoltic defects determines the initiation of vertebral failure*. The second was to establish the degree to which the failed vertebrae, having been allowed to recover under load simulating bed rest, retained residual load carrying capacity.

2. Methods

Fig. 1 presents an overview of the specimen preparation and mechanical testing work flow.

2.1. Specimen preparation

Five thoraco-lumbar spines were obtained from donors aged 65–78 years. Each spine was radiographed (Faxitron, HP, McMinnville, OR) to exclude existing pathology or fractures, the spine submerged in a saline bath to simulate soft tissues and Bone Mineral Density (BMD) measured in the anterior-posterior (A-P) and lateral (LAT) anatomical axis of the vetebra using a DXA scanner (QDR 2000+, Hologic Inc., Waltham, MA). Once dissected clean of all musculature, 18 individual vertebral levels were obtained by sectioning through the disc. The vertebrae were coded, wrapped in saline soaked gauze and stored at −20 °C in double plastic bags until the day of testing. Anterior (H_A) and posterior (H_P) vertebral body heights were measured from the sagittal radiographs and the measurement verified along the vertebral sagittal midline using a mechanical caliper (Mitutoyo, Japan, accuracy 0.01 mm). The location of the measurement was prescribed on the vertebra to be used for subsequent measurements (failed and recovered). For each stage (intact, failed and recovered) a vertebral deformity index (VDI) was computed from the following formula, $((H_P - H_A)/H_P)*100$.

2.2. Metastatic defect creation

On the day of testing, the vertebra was thawed for four hours at room temperature, followed by a one-hour submersion in a 37 °C heated saline bath. Registration markers, identifying the vertebral body sagittal and coronal anatomical axes, were created on the vertebral cortex and the vertebra registered to an imaging device secured to a fluoroscopy unit (Mini 6600, GE medical). Sagittal and coronal radiographs were obtained with care to keep magnification errors to a minimum, the images transferred to transparencies and the outlines of a defect, corresponding to 40 % of the vertebral body, drawn on the transferred images (Fig. 1). The drawings were super-imposed on the screens of the fluoroscopy unit and a high speed drill (MultiPro, Dremel, WI) with an attached 3 mm ball-end burring bit used to create an entry hole in the vertebral cortical shell with a diameter ranging from 6-9 mm, a mean of 7.2 mm (standard deviation = 1.4 mm). Under continuous fluoroscopy control, the drill was used to create a cavity in the vertebral body to match the one planned in the sagittal and coronal

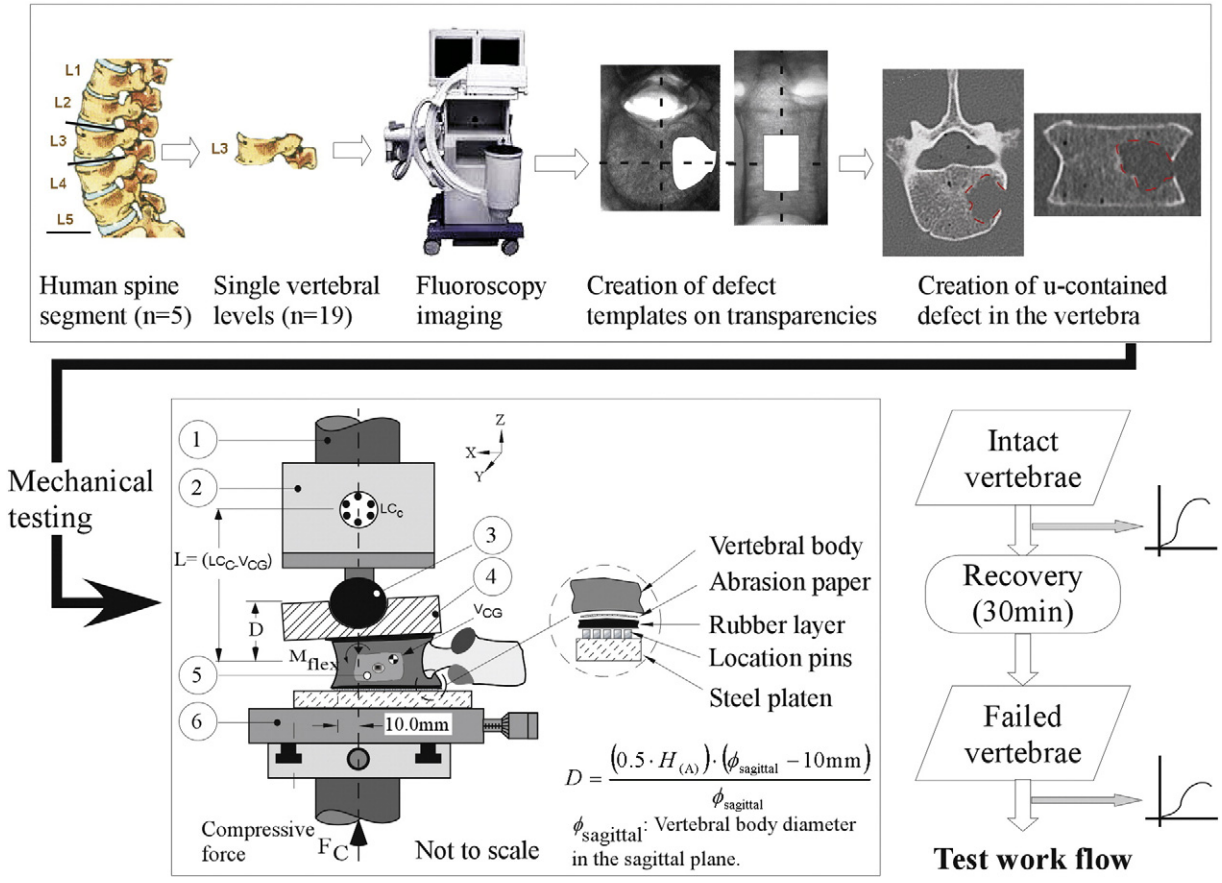

Fig. 1. A schematic diagram of the testing device used to apply combined compression and flexion loads onto the vertebral specimens. 3 mm rubber sheets located on either side of the vertebra allowed a more uniform transfer of load between the test device and the vertebra. Coarse-grit sandpaper, bonded on the outer side of the rubber sheets (Fig. 1) provided containment of the vertebra to the testing assembly whilst keeping the strengthening effect of cement embedding of the vertebra on the resulting vertebral deformations to a minimum. Required test displacement at the actuator, D, of the material testing system was computed from the equation (Alkalay et al., 2008) with ($H_{(A)}$): anterior height of the vertebra (intact, failed), $Ø_{sagittal}$: the sagittal diameter of the upper endplate measured from the X-rays.